FEBS Letters 588 (2014) 3409–3416

journal homepage: www.FEBSLetters.org

Zinc finger MYND-type containing 8 promotes tumour angiogenesis via induction of vascular endothelial growth factor-A expression

Junya Kuroyanagi [a,1], Yasuhito Shimada [a,b,c,d,e,1], Beibei Zhang [a], Michiko Ariyoshi [a], Noriko Umemoto [a,b], Yuhei Nishimura [a,b,c,d,e], Toshio Tanaka [a,b,c,d,e,*]

[a] Department of Molecular and Cellular Pharmacology, Pharmacogenomics and Pharmacoinformatics, Mie University Graduate School of Medicine, 2-174 Edobashi, Tsu, Mie 514-8507, Japan
[b] Department of Systems Pharmacology, Mie University Graduate School of Medicine, 2-174 Edobashi, Tsu, Mie 514-8507, Japan
[c] Mie University Medical Zebrafish Research Center, 2-174 Edobashi, Tsu, Mie 514-8507, Japan
[d] Department of Bioinformatics, Mie University Life Science Research Center, 2-174 Edobashi, Tsu, Mie 514-8507, Japan
[e] Department of Omics Medicine, Mie University Industrial Technology Innovation Institute, 2-174 Edobashi, Tsu, Mie 514-8507, Japan

ARTICLE INFO

Article history:
Received 4 May 2014
Revised 29 June 2014
Accepted 28 July 2014
Available online 10 August 2014

Edited by Beat Imhof

Keywords:
Prostate cancer
Tumour vessels
Xenotransplantation
Zebrafish
DNA microarray

ABSTRACT

Zinc finger, MYND-type containing 8 (ZMYND8) encodes a receptor for activated C-kinase protein. Here, we report that ZMYND8 promotes angiogenesis in prostate cancer xenografts in zebrafish, as well as tube formation in human umbilical vascular endothelial cell (HUVEC) cultures. Using transcriptome analyses, we found upregulation of ZMYND8 expression in both zebrafish prostate cancer xenografts and prostate cancer samples from patients. In vitro and in vivo ZMYND8 knockdown suppressed angiogenesis, whereas ZMYND8 overexpression enhanced angiogenesis. Notably, ZMYND8 induced *vegfa* mRNA expression selectively in prostate cancer xenografts. Integrated analysis of human and zebrafish transcriptomes, which identified *ZMYND8*, might be a powerful strategy to determine also other molecular targets for inhibiting prostate cancer progression.

1. Introduction

Because tumour-associated angiogenesis is crucial for solid malignancies including prostate cancer, inhibition of tumour neovascularization and/or destruction of tumour vasculature might maintain tumours in a dormant state or, in combination with cytotoxic therapies, may potentiate tumour shrinkage. Molecular targeted agents (mainly antagonists of vascular endothelial growth factor [VEGF] pathways) have been developed to block proangiogenic signal transduction. For example, bevacizumab, a humanized antibody against VEGF-A, was the first antiangiogenic agent to be approved for treatment of several advanced cancers [1]. Furthermore, sunitinib, a small molecule that blocks intracellular VEGF, KIT, Flt3, and platelet-derived growth factor receptors, regulates angiogenesis and cell growth, and has been approved for treatment of advanced renal cell cancer and malignant gastrointestinal stromal tumours [2]. However, there are still a limited number of target molecules to inhibit cancer progression including tumour angiogenesis and metastasis. To overcome this limitation, several approaches based on screening and omics technologies together with animal modelling have been developed for target discovery and validation.

Various animal models have been established to investigate angiogenic processes and identify proangiogenic and antiangiogenic compounds. Over the last few decades, the zebrafish as a disease model has emerged as a high throughput and cost effective alternative to other animal models, which has been used to assess the efficacy and toxicity of several chemical compounds [3,4]. In cancer research, xenografts of various cancer cell lines induce neovascularization in zebrafish [5–8]. Furthermore, a high degree of conservation of the pathways involved in tumourigenesis, angiogenesis, and metastasis has been proven in zebrafish and mammals [9,10]. Zebrafish also present powerful imaging solutions through in vivo fluorescent labelling of desired organs such as the vasculature system in combination with their body wall transparency [11]. Because the zebrafish is exploitable for genome-wide, loss-of-function analyses, we used human cancer-xenografted zebrafish in

* Corresponding author at: Department of Molecular and Cellular Pharmacology, Pharmacogenomics and Pharmacoinformatics, Mie University Graduate School of Medicine, 2-174 Edobashi, Tsu, Mie 514-8507, Japan. Fax: +81 59 232 1765.
E-mail address: tanaka@doc.medic.mie-u.ac.jp (T. Tanaka).
[1] Junya Kuroyanagi and Yasuhito Shimada contributed equally to this work.

http://dx.doi.org/10.1016/j.febslet.2014.07.033
0014-5793/

combination with DNA microarray analysis and morpholino antisense oligonucleotide (MO) knockdown, and found a new therapeutic target, zinc-finger MYND-type containing 8 (zmynd8), for inhibition of tumour angiogenesis.

2. Materials and methods

An expanded Methods section is available in the online-only Data Supplement.

2.1. Ethics approval

This study was approved by the Ethics Committee of Mie University. The procedures were performed according to the Japanese animal welfare regulation 'Act on Welfare and Management of Animals' (Ministry of Environment, Japan) and complied with international guidelines.

2.2. Chemicals

LY317615 and Ly333531 were purchased from Selleck Chemicals (Houston, TX, USA) and Tocris Bioscience (Bristol, UK), respectively. Stock solutions (10 mM) were prepared by dissolving the chemicals in dimethyl sulfoxide (Sigma–Aldrich, St. Louis, MO, USA). For anaesthesia, 100 ppm 2-phenoxyethanol (2-PE; Tokyo Kasei, Tokyo, Japan) was diluted in E3 medium (5 mM NaCl, 0.17 mM KCl, 0.4 mM $CaCl_2$, and 0.16 mM $MgSO_4$).

2.3. Zebrafish

The care and breeding of zebrafish followed previously described protocols [12]. Because of the transparency of their bodies, which facilitates in vivo monitoring of tumour angiogenesis, *nacre/fli1:egfp* zebrafish obtained by cross-breeding *nacre* mutants [13] and *fli1:egfp* transgenic zebrafish [11] were used in the experiments. At 3 days prior to xenotransplantation, individual female zebrafish were placed in mating tanks with males. The next morning, mating was initiated by light stimuli, followed by collection of the resulting fertilized eggs. The eggs were incubated in E3 medium at 28 °C. Preceding xenotransplantation, 48 h post-fertilization (hpf) embryos were dechorionated using a 2 mg/ml pronase solution (Roche Diagnostics, Mannheim, Germany) as described previously [12]. After dechorionation, the embryos were anaesthetized by immersion in 100 ppm 2-PE. Then, the embryos were arrayed onto an embryo-holding sheet for xenotransplantation procedures.

2.4. DU145-Kusabira orange (KOr) cell xenotransplantation

DU145 human prostate cancer cells were obtained from the RIKEN Cell Bank (Tokyo, Japan), and DU145 cells stably expressing Kusabira orange (KOr) (DU145-KOr cells) were established as described in Supplementary Methods. DU145-KOr xenotransplantation was conducted according to a previous report [8] with some modification. DU145-KOr cells (1×10^6 cells) were suspended in 30 μl Matrigel (BD Biosciences, San Jose, CA, USA) at 4 °C. The glass needles used to inject the cells were prepared from GD-1 glass capillaries (Narishige, Tokyo, Japan) using a PP-830 gravity puller (Narishige) and finely polished with an EG-44 microforge (Narishige). The avascular region of the yolk sac was then injected with 10 nl of the cell suspension containing 100–200 cells using a glass needle and FemtoJet injection system (Eppendorf, Hamburg, Germany). The xenografted zebrafish were subsequently incubated in E3 medium at 32 °C. At 48 hpi, 80–90% of the injected zebrafish exhibited tumours in their yolk sac.

2.5. Imaging of xenotransplants in zebrafish

Zebrafish were anesthetised with 100 ppm 2-PE. Images were then captured under a MZ16F stereoscopic microscope (Leica Microsystems, Wetzlar, Germany) equipped with a DP71 digital camera (Olympus, Tokyo, Japan). For fluorescence imaging, we used GFP2 (for fli1:egfp) and DsRed (for KOr) filters. Tumour cell proliferation was calculated by the ratio of the KOr fluorescence intensity in the tumour area with ImageJ software (National Institutes of Health, Bethesda, MD, USA) as described previously [14].

2.6. cDNA synthesis and quantitative RT-PCR (qRT-PCR)

Total RNA was extracted from DU145-xenografted zebrafish at 48 h post-implantation (hpi) using Trizol reagent (Life Technologies, Carlsbad, CA, USA) in combination with a cleanup protocol (RNeasy Mini Kit; Qiagen, Hilden, Germany). First-strand cDNA was synthesized from 200 ng total RNA using a Super Script III cDNA synthesis kit (Life Technologies) and random primers (Life Technologies). qRT-PCR was performed using Power SYBR Green Master Mix (Applied Biosystems, Foster City, CA, USA) and a 7300 real-time PCR system (Applied Biosystems) as recommended by the manufacturer. The target gene was amplified using the primers shown in Table S1. Data were normalized to the mRNA level of beta-2-microglobulin (human B2M, NM_004048; zebrafish b2m, NM_001159768).

2.7. DNA microarrays

Total RNA was extracted from DU145-xenografted zebrafish at 48 hpi with or without tumour angiogenesis as described above. The samples for each condition were obtained from three independent experiments. Each experimental group included 5–10 xenografts. Detailed methods for the DNA microarray analysis are described in Supplementary Methods.

2.8. MOs

Based on the cDNA sequences in GenBank for zebrafish zmynd8 (XM_687794) and vascular endothelial growth factor aa (vegfaa) (NM_131498), MOs against zfZMYND8 (zfZMYND8 MO) and zfVEGFAa (zfVEGFAa MO) were synthesized by Gene Tools (Philomath, OR, USA). For the negative control, we used a control MO (human β-globin mutant sequence; GeneTools). The MO sequences are shown in Table S1. Each MO was injected into the yolk sac (48 hpf) with or without DU145-KOr cells using a fine glass needle connected to the FemtoJet automatic injector. To confirm the MO distribution, we injected lissamine-conjugated control MO (GeneTools) into 48 hpf embryos (Fig. S1). One hundred picoliters of 100 μM MO in water was injected in accordance with a previous report [15].

2.9. ZMYND8 mRNA synthesis and rescue

pCMV-SPORT6.1 carrying full-length human ZMYND8 cDNA was obtained from Open Biosystems (Huntsville, AL, USA) and subcloned into a pTnT vector (Promega, Madison, WI, USA). The full-length human ZMYND8 cDNA was then amplified by PCR, and the PCR products were used as templates for RNA synthesis. ZMYND8 mRNA was synthesized using a mMessage mMachine transcription kit for T7 RNA polymerase (Ambion, Austin, TX, USA). For the rescue experiment, a solution containing 0.5 ng/nl ZMYND8 mRNA and 8 ng zfZMYND8-MO was injected into 48 hpf embryos with xenotransplants.

3. Results

3.1. Transcriptome analyses reveal an increase in zmynd8 expression during tumour angiogenesis

DU145-KOr cell implantation into the avascular region of the yolk sac of 48 hpf zebrafish induced tumour angiogenesis in 34% of the xenografted animals at 48 hpi (of the 124 injected zebrafish eggs, 107 developed tumours [xenografted] and 36 of these xenografted zebrafish underwent tumour angiogenesis). The tumour vessels were elongated from common caudal veins and/or subintestinal veins surrounding the implanted cancer cells, which were not observed in control zebrafish (Fig. 1A). Tumour sizes were significantly increased in the angiogenesis (+) group ($P < 0.05$; Fig. 1B), suggesting that the tumour vessels contributed to cancer cell proliferation in DU145-KOr xenografts.

DNA microarray analyses were performed using total RNA from DU145-xenografted zebrafish. In the tumour angiogenesis (+) group, 36 and 172 genes showed significantly (false positive rate [FDR]<0.1) decreased or increased expression, respectively, compared with that in the angiogenesis (−) group (Table S2). Blast analyses [16] revealed that the zebrafish genes with decreased or increased expression represented 17 and 96 human orthologs, respectively. Analysis of these genes by Gene Ontology (GO) terms using GOstat [17] revealed that 16.8% and 9.7% of their human orthologs are involved in apoptosis and protein kinase activity, respectively (Table S3). To determine the genes responsible for tumour angiogenesis, we analysed the transcriptome data of human clinical samples, [GSE3325 [18], GSE6605 [19], GSE6919 [20], and GSE27616 [21]], and our zebrafish DNA microarray data. Among these data, the expression of three genes was significantly (FDR < 0.1) increased or decreased during cancer progression compared with that in normal tissues (Table 1). Of the three genes, qRT-PCR analyses confirmed the DNA microarray results indicating that *zmynd8* expression was increased by almost 4-fold during tumour angiogenesis compared with that in the non-xenografted control and angiogenesis (−) group ($P < 0.01$; Fig. 1C). Zebrafish zmynd8 protein shows 67% similarity and 77% identity with human ZMYND8 in BLAST analysis [22]. While the similarity of the amino acid sequences is moderate in zebrafish and human ZMYND8 proteins, the similarity in each functional domain (zinc finger domain at the N-terminus, bromodomain, PWWP domain, and zinc finger MYND-type domain) is very high (88–100%; Fig. S2). This finding indicates that the pathophysiological function of ZMYND8 would be highly conserved in vertebrates. Notably, human *ZMYND8* mRNA was also increased during tumour angiogenesis ($P < 0.01$; Fig. 1C). To determine whether the protein levels of ZMYND8 were also altered in prostate cancers, we conducted immunohistochemistry using human prostate cancer tissue microarrays (Fig. 1D). In normal prostate, ZMYND8 was expressed in glandular and vascular epithelia, but not in connective tissues. In prostate cancer tissues, ZMYND8 was expressed in cancer cells, but not in stromal cells. Human ZMYND8 expression was increased at the neoplastic stage ($P < 0.01$ vs. normal prostate tissues), and particularly at the metastatic stage IV ($P < 0.05$ vs. stage I; Fig. 1E).

3.2. ZMYND8 regulates tumour angiogenesis in DU145-xenografted zebrafish

To analyse the role of zebrafish zmynd8 in tumour angiogenesis, we co-injected zfZMYND8 MO and DU145-KOr cells into zebrafish at 48 hpf. As a result, zfZMYND8 MO decreased the expression of zmynd8 protein ($P < 0.05$ vs. control MO; Fig. 2A and B). Similar to co-injection of vegfab MO (zfVEGFAb MO) as the positive control (Fig. S3), zfZMYND8 MO co-injection with DU145-KOr cells suppressed tumour angiogenesis (Fig. 2C). Furthermore, the frequency of tumour angiogenesis was suppressed significantly ($P < 0.05$; Fig. 2D), while the tumour size was not changed by zfZMYND8 MO (Fig. 2E). Yolk sac injection of these MOs at 48 hpf did not alter physiological angiogenesis at 96 hpf (Fig. S4). Because the

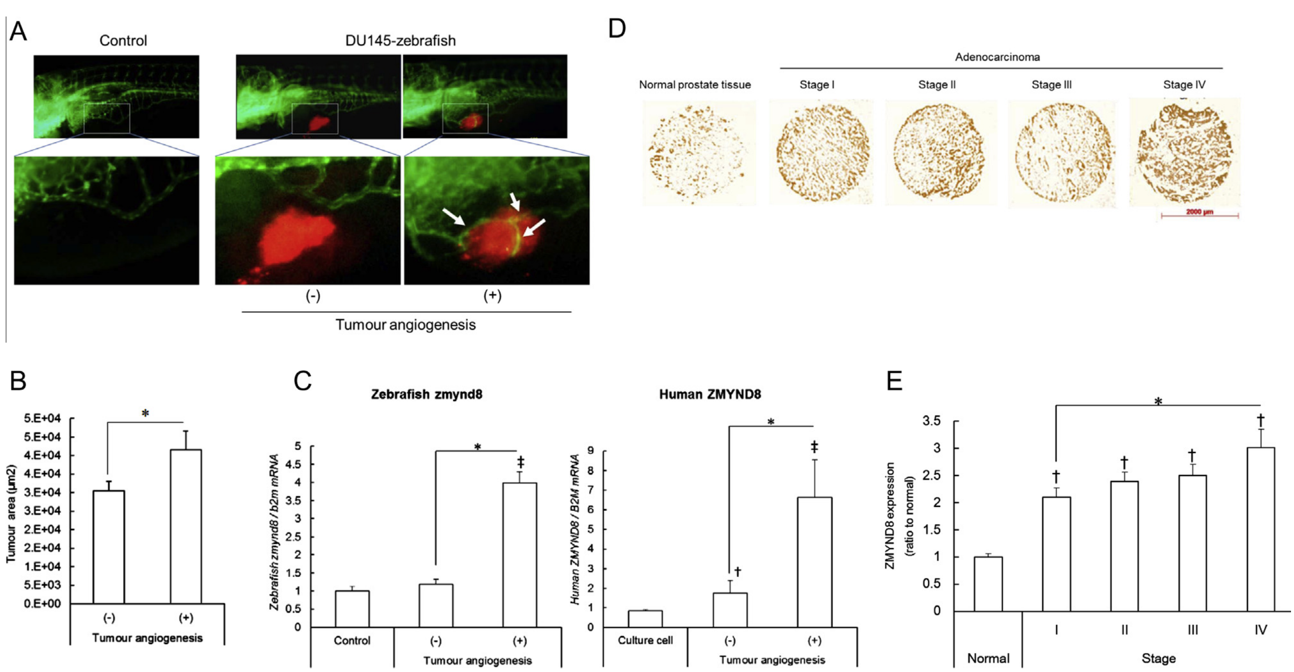

Fig. 1. ZMYND8 expression increases during cancer progression. (A) Typical images of DU145-xenografted zebrafish. Arrow indicates tumour vessels. Almost 34% of DU145-xenografted zebrafish exhibited tumour angiogenesis. The lower images are enlarged views of the outlined areas. White arrows indicate tumour vessels. (B) The tumour size was increased in tumour angiogenesis (+) zebrafish at 96 hpf. $n = 12$, $^{*}P < 0.05$. (C) Zebrafish *zmynd8* (left) and human *ZMYND8* (right) mRNA expression was increased in DU145 xenografts with tumour angiogenesis. $n = 5$, $^{*}P < 0.01$, $^{\dagger}P < 0.05$ and $^{\ddagger}P < 0.01$ vs. control (no xenograft or cultured cells, respectively). (D) *ZMYND8* mRNA expression in clinical prostate cancer specimens (GSE3324 and GSE6909). $n = 6$–7, $^{*}P < 0.05$, $^{**}P < 0.01$ vs. normal tissue. $^{*}P < 0.05$. GSE3324 and GSE6909 include 6–7 and 18–25 specimens at each stage, respectively. (E) Immunostaining of human ZMYND8 in clinical prostate cancer specimens. $n = 3$–7, $^{*}P < 0.05$ vs. stage I, $^{\dagger}P < 0.01$ vs. normal tissue.

Table 1
Genes with altered expression in zebrafish and human prostate cancer progression.

Gene symbol	Zebrafish xenograft		Human prostate cancer (GSE3325)		Human prostate cancer (GSE6605)		Human prostate cancer (GSE6919)		Human prostate cancer (GSE27616)	
	Log2 ratio	FDR	Log2 ratio	FDR	Log2 ratio	FDR	Log2 ratio	FDR	Log2 ratio	FDR
TARS	2.47	0.01	1.18	0.01	0.54	0.02	1.84	0	0.03	0.78
ZMYND8	1.33	0.02	1.51	0.02	1.49	0	1.78	0	0.71	0.00
IRF7	1.21	0.02	1	0.04	1.73	0	0.81	0	0.00	0.97

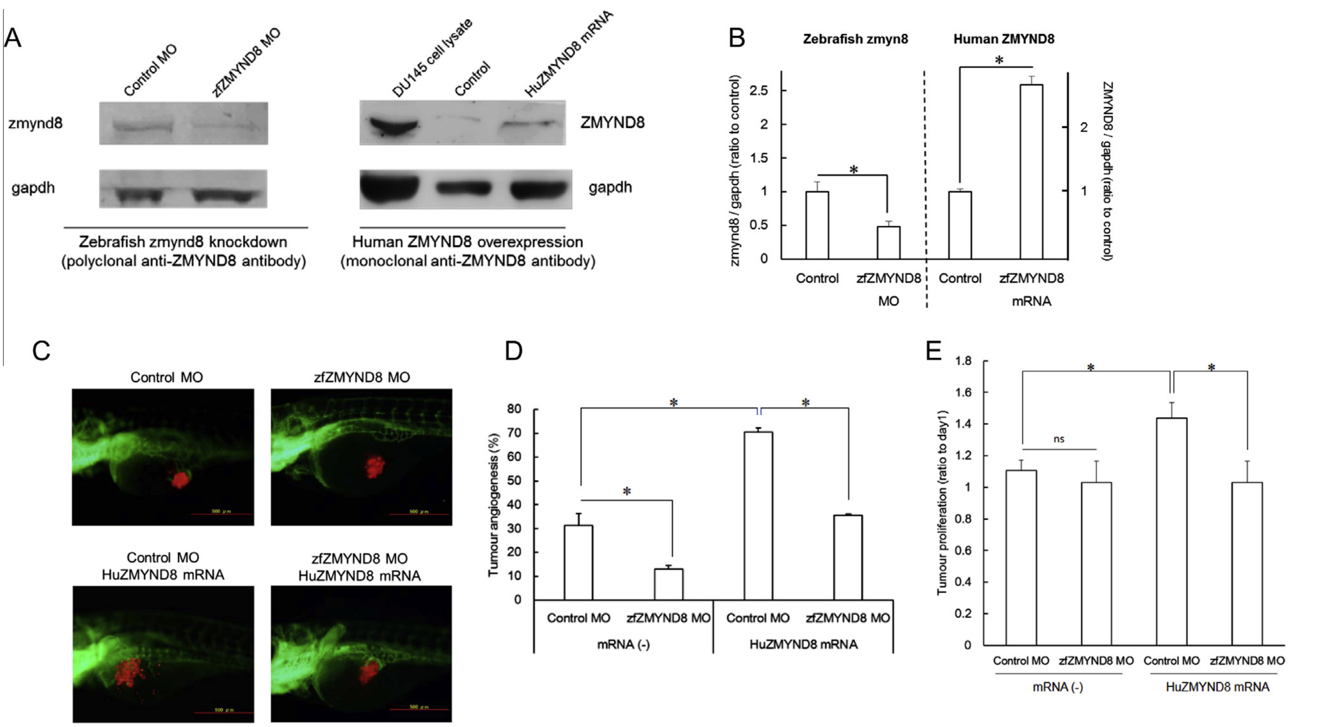

Fig. 2. ZMYND8 is involved in tumour angiogenesis. (A) Western blot of control zebrafish injected with zfZMYND8 MO or HuZMYND8 mRNA at 48 hpf. The lysate was prepared at 96 hpf. (B) Densitometric analysis of (A). Compared with the control MO, zfZMYND8 MO decreased zmynd8 protein expression to 50%, whereas HuZMND8 mRNA increased ZMYND8 protein expression by 2.5-fold compared with that in the control. $n = 3–4$, $^{*}P < 0.05$. (C) Typical images of zfZMYND8 MO and human ZMYND8 rescue in DU145-xenografted zebrafish at 96 hpf. zfZNYND8 MO suppressed tumour angiogenesis and HuZMYND8 mRNA rescued the effect of zfZNYND8 MO. (D) Frequency analysis of (C). Tumour angiogenesis was decreased and increased by zfZMYND8 MO and HuZMYND8 mRNA, respectively. $n = 3$, $^{*}P < 0.05$. Each experimental group included 27–49 zebrafish. (E) Tumour proliferation of (C). $n = 91–114$, $^{*}P < 0.05$.

complete zebrafish zmynd8 cDNA sequence is unavailable, we conducted human *ZMYND8* (*HuZMYND8*) mRNA rescue (Fig. 2A). As shown in Fig. 2C and D, *HuZMYND8* mRNA co-injection promoted tumour angiogenesis with or without zebrafish *zmynd8* knockdown. Because of the differences in the amino acid sequences of zfZMYND8 and HuZMYND8, zfZMYND8 MO could not suppress the translation of HuZMYND8 mRNA. Therefore, the zfZMYND8 MO-induced reduction of tumour angiogenesis was recovered by introduction of HuZMYND8 mRNA. Consequently, the tumour size of xenotransplanted cancer cells was increased significantly ($P < 0.05$; Fig. 2E).

3.3. ZMYND8 knockdown suppresses tube formation of human umbilical vein endothelial cells (HUVECs)

To evaluate the functional similarity between human and zebrafish ZMYND8, we conducted capillary tube formation experiments using HUVECs with siRNA-mediated knockdown of Human ZMYND8 (Fig. 3A). Human ZMYND8 knockdown did not affect HUVEC proliferation (Fig. 3B), but their capacity for tube formation was drastically suppressed by all ZMYND8 siRNAs ($P < 0.01$; Fig. 3C and D). These results are consistent with those of zebrafish xenograft experiments (Fig. 2).

3.4. Human ZMYND8 in DU145-KOr cells regulates tumour growth in DU145-xenografted zebrafish

The expression of human ZMYND8 was increased in tumour xenografts (Fig. 1C) and human clinical samples (Fig. 1D,E and Table 1). Therefore, we conducted xenotransplantation with *ZMYND8* knockdown or overexpression in DU145-KOr cells (Figs. 4A and S5). Similar to the results obtained with HUVECs (Fig. 3B), *ZMYND8* knockdown or overexpression did not affect DU145-KOr cell proliferation (Figs. 4B and S6). In contrast to zebrafish zmynd8 knockdown, DU145-KOr cells with *ZMYND8* knockdown had no effect on tumour angiogenesis in xenografted zebrafish, whereas *ZMYND8* overexpression increased tumour angiogenesis (Fig. 4C and D). The sizes of the tumour xenografts were also increased by *ZMYND8* overexpression, which corresponded to tumour angiogenesis (Fig. 4E).

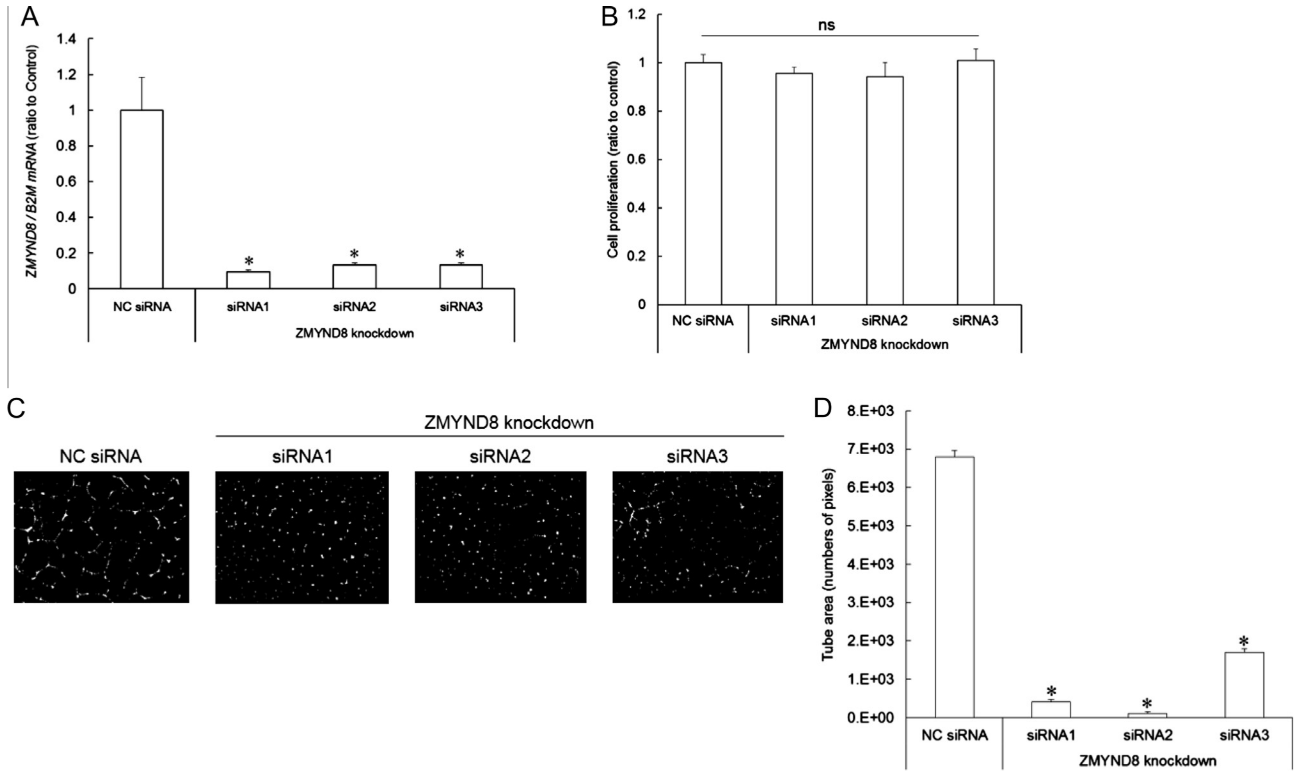

Fig. 3. Human ZMYND8 knockdown suppresses tube formation. (A) ZMYND8 siRNA transfection of HUVECs. *ZMYND8* knockdown was confirmed by qRT-PCR. $n = 4$, $^*P < 0.01$. (B) *ZMYND8* knockdown did not affect HUVEC proliferation. $n = 8$. (C) *ZMYND8* knockdown suppressed tube formation of HUVECs. (D) Quantitative analysis of (C). A decrease in the tube area was induced by each ZMYND8 siRNA. $n = 8$, $^*P < 0.01$ vs. NC siRNA.

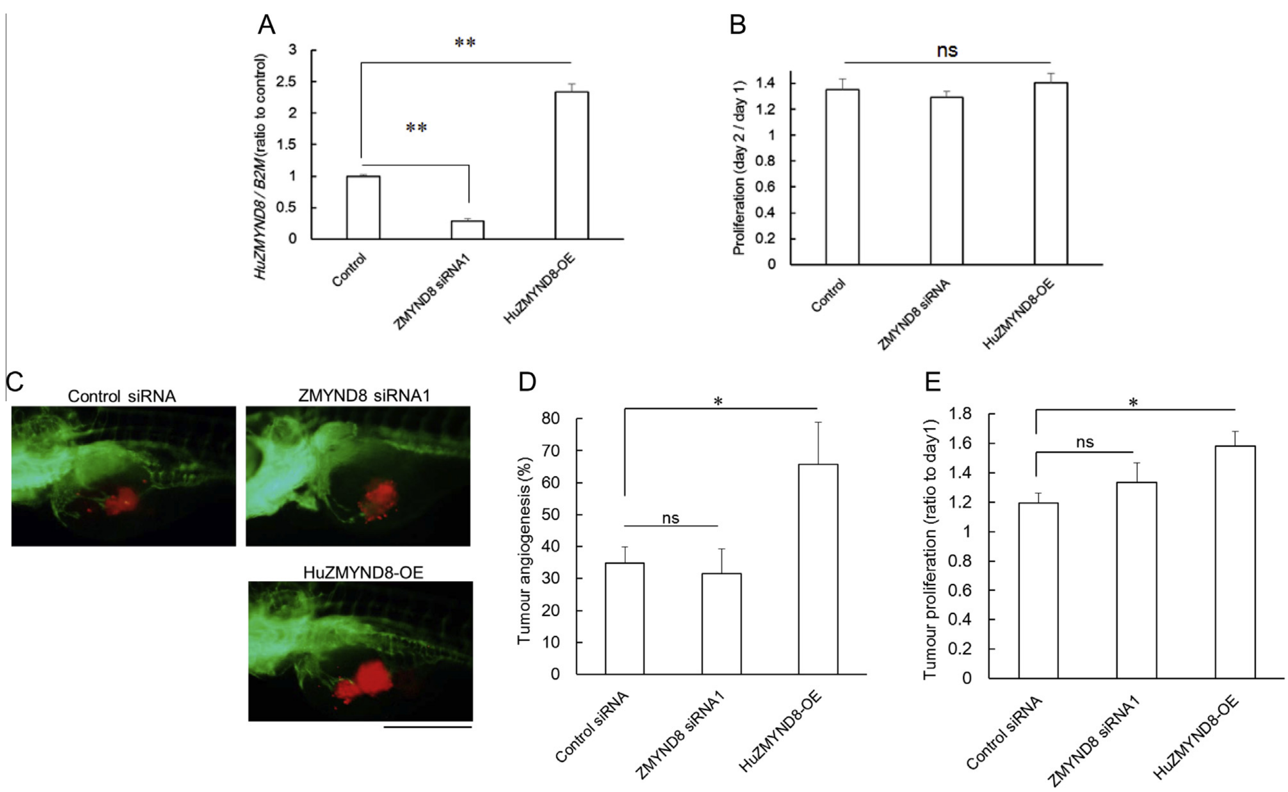

Fig. 4. Human ZMYND8 modulation in DU145-KOr cells. (A) Human *ZMYND8* knockdown (ZMYND8 siRNA) and overexpression (HuZMYND8-OE) in DU145-KOr cells were confirmed by qRT-PCR. $n = 3–4$, $^{**}P < 0.01$. (B) *ZMYND8* modulation did not affect DU145-KOr cell proliferation. $n = 8$. (C) Typical images of ZMYND8-modulated DU145-xenografted zebrafish. (D) Angiogenesis frequency analysis of ZMYND8-modulated DU145-KOr cell xenotransplantation. HuZMYND8-OE increased tumour angiogenesis in DU145-xenografted zebrafish at 48 hpi. $n = 3$, $^*P < 0.05$. Each experimental group included 17–25 zebrafish. (E) Tumour cell proliferation of (D). $n = 53–67$, $^*P < 0.05$.

3.5. ZMYND8 induces tumour angiogenesis via vegfa expression

Because hypoxia promotes pathophysiological angiogenesis in several diseases including cancer, we conducted hypoxic treatment of developing zebrafish. As shown in Fig. S7, *zmynd8* expression was induced together with *hypoxia-inducible factor 1* (*hif1a*), *vegfaa*, *vegfab*, and *vegfc* under hypoxic conditions at 72 hpf. To investigate the relationship between ZMYND8 and VEGF signalling, we conducted qRT-PCR analysis of *vegf* isoforms and receptors in DU145-xenografted zebrafish treated with zfZMYND8 MO and HuZNYND8 mRNA (Fig. 5). As a result, zmynd8 regulated the expression of *vegfaa and vegfab* isoforms ($P < 0.05$ vs. DU145-xenografted zebrafish; Fig. 5A and B), but not *vegfc* (Fig. 5C). In addition, zfZMYND8 MO did not suppress the expression of vegf receptors, whereas HuZMYND8 mRNA induced significant expression of vegf receptors *flt1* (Fig. 5D), *kdr* (Fig. 5E), and *flt4* (Fig. 5F) ($P < 0.05$ vs. DU145-xenografted zebrafish).

To examine gene modulation by ZMYND8 in DU145-KOr cells, qRT-PCR analyses of zebrafish xenografts revealed that *ZMYND8* overexpression slightly increased *VEGFA* expression in cultured cells (Fig. 5G). However, *ZMYND8* overexpression in DU145 cells did not increase expression of the corresponding zebrafish orthologs (*vegfaa* and *vegfab*) in tumour xenografts (Fig. 5H). In summary, the role of ZMYND8 in tumour angiogenesis of DU145 xenografts depends mainly on the surrounding zebrafish tissues that regulate *vegfa* transcription.

4. Discussion

ZMYND8 was initially identified as a receptor for activated C-kinase (RACK) protein that binds to activated protein kinase C beta I (PKCβI) [23]. In cancer research, ZMYND8 has been reported to be a cutaneous T-cell lymphoma-associated antigen [24]. Recently, a ZMYND8-RELA fusion gene was found to increase leukaemogenically via the NF-κB pathway in acute erythroid leukaemia [25]. ZMYND8 mutation has the highest frequency (19%) in patients with colorectal cancers [26]. The copy numbers of ZMYND8 are also increased by 2–3-fold in several cancer cell lines (Table S4), according to the canSAR database (The Institute of Cancer Research, London, UK) and catalogue of somatic mutations in cancer (COSMIC; Welcome Trust Sanger Institute, Cambridge, UK). These studies indicate that ZMYND8 is involved in cancer progression, but the pathophysiological function of ZMYND8 remains unknown.

In the current study, we discovered that ZMYND8 promotes tumour angiogenesis and contributes to cancer cell proliferation. One of the major factors for tumour angiogenesis is hypoxia, and we found that hypoxia promoted *zmynd8* expression in zebrafish (Fig. S7). An *in silico* promoter sequence analysis using Pattern Search for Transcriptional Factor Binding Site (PATCH, public 1.0; Biobase, Wolfenbuettel, Germany) revealed that human and zebrafish ZMYND8 promoters (3000 bp downstream from the start codon) have 10 and seven possible HIF1-binding sites, respectively (Fig. S8), which corresponds to our in vivo results. Based on these results, zmynd8 would be downstream of HIF-1, which is similar to another RACK family protein, RACK1 [27]. RACK1 binds to Flt1 (VEGF receptor type 1) directly and regulates the PI3K-Akt-Rac1 pathway in CLL cell migration [27] and hypoxia-induced angiogenesis in breast cancer cells [28]. The functional similarity of ZMYND8 and RACK1 for binding to VEGFRs may exert a hypoxia-induced angiogenic response. However, ZMYND8 and RACK1 belong to different protein families, and the sequence similarity of ZMYND8 and RACK1 is quite low (human: 13.2%; zebrafish: 12.9%).

PKC isozymes, in particular PKCβ, a binding partner of ZMYND8, are important mediators of VEGF signalling, and their inhibition leads to decreased endothelial cell proliferation and a reduction in neovascularization of malignant tumours [29,30]. Although a

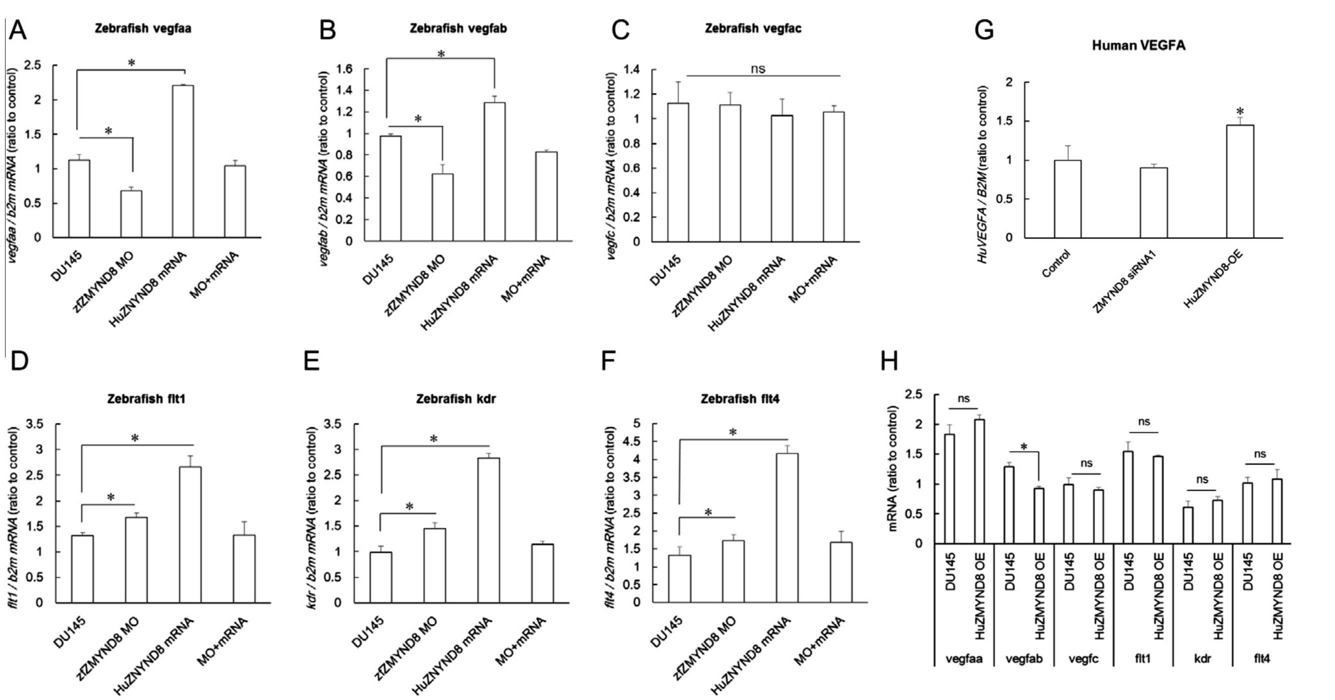

Fig. 5. Quantitative RT-PCR analyses of genes involved in the VEGF pathway of ZMYND8-modulated xenografts in zebrafish. (A–C) Expression of *vegf* mRNAs in *zmynd8*-modulated, DU145-xenografted zebrafish. Zebrafish *zmynd8* modulation altered the expression of *vegfaa* (A) and *vegfab* (B) mRNAs, but not *vegfc* mRNA (C). $n = 4$, $^{*}P < 0.05$. (D–F) Expression of zebrafish *vegf receptors* in *zmynd8*-modulated, DU145-xenografted zebrafish. Zebrafish *zmynd8* modulation increased *flt1* (D), *kdr* (E), and *flt4* (F) mRNA expression. $n = 4$, $^{*}P < 0.05$. (G) Expression of *VEGFA* mRNA in ZMYND8-modulated, DU145-KOr-xenografted zebrafish. *ZMYND8* overexpression in DU145-KOr cells (HuZMYND8-OE) increased *ZMYND8* mRNA expression in DU145-xenografted zebrafish. $n = 4$, $^{*}P < 0.05$. (H) HuZMYND8-OE did not alter the expression of genes involved in the vegf pathway of zebrafish. $n = 4$, $^{*}P < 0.05$.

PKCβ inhibitor, LY317615 (enzastaurin), is undergoing clinical trials for several malignancies [31–34], the high degree of sequence homology and structural similarity of the catalytic regions among PKC isozymes and other protein kinases suggest that development of isozyme-selective inhibitors will be extremely challenging [35]. In addition, because multiple PKC isozymes are expressed in all cell types throughout the body, which perform crucial roles in normal physiology, systemic inhibition of PKCs may result in undesired on-target side effects such as delayed wound healing [36]. We also evaluated PKCβ inhibitors Ly317615 and Ly333531 in the xenograft zebrafish model. When these chemicals were exposed to normal zebrafish at 3–8 dpf, there was a drastic decrease in their survival rate (Fig. S9). In tumour xenografts, the maximum tolerable concentration of each PKCβ inhibitor (Ly317615: 1 μM; Ly333531: 3 or 10 μM) could not suppress tumour angiogenesis at 3 dpi (Fig. S10). To overcome these limitations, a new class of PKC modulator has been developed to inhibit protein–protein interactions that are crucial for PKC activation, including those with RACK proteins, because of their high binding specificity for PKC isozymes [36]. For example, βIIV5-3, an inhibitor of PKCβII-RACK1 binding [37], prevents neovascularisation in a xenograft mouse model of prostate cancer [38]. Based on our results, inhibition of ZMYND8 (previously known as RACK7) as a co-effector of PKCβI [23] appears to be a promising approach to modulate PKCβI activity in the neovascularisation of prostate cancer progression in the same context. In addition to the direct interaction of ZMYND8 with PKCβI, ZMYND8 binds to formin homology-2-domain containing protein 1 [39] that has several potential PKC phosphorylation domains [40]. This finding suggests that ZMYND8 regulates PKCβ phosphorylation and activity as a component of the PKC regulatory complex. As a PKCβ modulator, ZMYND8 may be a suitable drug target for inhibition of tumour angiogenesis.

In the current study, zmynd8 regulated *vegfa* expression during tumour angiogenesis. Many studies have reported that the PKC pathway is downstream of VEGF-VEGFR signalling. However, PKC isozymes are also known to induce VEGFA mRNA expression in several angiogenic diseases, including cancers, and *vice versa* [41] [42]. Considering these observations, ZMYND8 plays a key regulatory role in pathological angiogenesis, probably by contributing to the PKCβ-VEGFA axis. In our zebrafish model, ZMYND8 knockdown could not suppress tumour proliferation (Fig. 2E), despite inhibition of angiogenesis (Fig. 2D). Drabsch et al. proposed that cancer xenografts in zebrafish highlight the effects at the early stages of tumour development [43]. Thus, our results indicate that the early stage of tumour proliferation was not suppressed by inhibition of angiogenesis, which is similar to the early stage (~2 mm) of human cancer [44]. In addition, ZMYND8 knockdown in cancer cells could not suppress tumour angiogenesis (Fig. 4C). However, zmynd8 knockdown in zebrafish suppressed tumour angiogenesis (Fig. 2D), corresponding to the results showing that human ZMYND8 knockdown could not reduce VEGFA expression (Fig. 5G). These results indicate a pathway for tumour angiogenesis (mainly VEGF signalling), which compensates for human ZMYND8 knockdown in cancer cells but not their surrounding tissues. ZMYND8 expression was increased in cancer cells and tumour vessels, but the pathological role of these inductions would be different.

In summary, we show that *ZMYND8* is one of the contributing factors in tumour angiogenesis via *VEGFA* expression. *zmynd8* knockdown zebrafish show no obvious phenotypic changes (Fig. S4), suggesting that ZMYND8 may be a novel therapeutic target to inhibit cancer progression without on-target side effects. The combination of in vivo, in vitro, and in silico data will hopefully lead to the use of ZMYND8 as a therapeutic target for treatment of progressive cancers.

Financial support

This work was supported in part by the Japan Science and Technology Agency, New Energy and Industrial Technology Development Organization, and the Yokoyama Rinsho Foundation, Japan.

Conflict of interest

The authors declare that they have no conflicts of interest.

Acknowledgments

We thank S. Ichikawa for experimental assistance, A. Suzuki for zebrafish breeding and maintenance, and R. Ikeyama and Y. Tamura for secretarial assistance. This work was supported in part by the Japan Science and Technology Agency, New Energy and Industrial Technology Development Organization, and Yokoyama Rinsyo Foundation, Japan.

Appendix A. Supplementary data

Supplementary data associated with this article can be found, in the online version, at http://dx.doi.org/10.1016/j.febslet.2014.07.033.

References

[1] Glade-Bender, J., Kandel, J.J. and Yamashiro, D.J. (2003) VEGF blocking therapy in the treatment of cancer. Expert Opin. Biol. Ther. 3, 263–276.
[2] Motzer, R.J., Hoosen, S., Bello, C.L. and Christensen, J.G. (2006) Sunitinib malate for the treatment of solid tumours: a review of current clinical data. Expert Opin. Investig. Drugs 15, 553–561.
[3] Zon, L.I. and Peterson, R.T. (2005) In vivo drug discovery in the zebrafish. Nat. Rev. Drug Discov. 4, 35–44.
[4] Jing, L. and Zon, L.I. (2011) Zebrafish as a model for normal and malignant hematopoiesis. Dis. Model Mech. 4, 433–438.
[5] Feitsma, H. and Cuppen, E. (2008) Zebrafish as a cancer model. Mol. Cancer Res. 6, 685–694.
[6] Nicoli, S., Ribatti, D., Cotelli, F. and Presta, M. (2007) Mammalian tumor xenografts induce neovascularization in zebrafish embryos. Cancer Res. 67, 2927–2931.
[7] Stoletov, K., Montel, V., Lester, R.D., Gonias, S.L. and Klemke, R. (2007) High-resolution imaging of the dynamic tumor cell vascular interface in transparent zebrafish. Proc. Natl. Acad. Sci. USA 104, 17406–17411.
[8] Nicoli, S. and Presta, M. (2007) The zebrafish/tumor xenograft angiogenesis assay. Nat. Protoc. 2, 2918–2923.
[9] Tobia, C., Gariano, G., De Sena, G. and Presta, M. (2013) Zebrafish embryo as a tool to study tumor/endothelial cell cross-talk. Biochim. Biophys. Acta 1832, 1371–1377.
[10] Konantz, M., Balci, T.B., Hartwig, U.F., Dellaire, G., André, M.C., Berman, J.N. and Lengerke, C. (2012) Zebrafish xenografts as a tool for in vivo studies on human cancer. Ann. NY Acad. Sci. 1266, 124–137.
[11] Lawson, N.D. and Weinstein, B.M. (2002) In vivo imaging of embryonic vascular development using transgenic zebrafish. Dev. Biol. 248, 307–318.
[12] Westerfield, M. (2007) A Guide for the Laboratory use of Zebrafish (*Danio rerio*), The Zebrafish Book.
[13] Lister, J.A., Robertson, C.P., Lepage, T., Johnson, S.L. and Raible, D.W. (1999) Nacre encodes a zebrafish microphthalmia-related protein that regulates neural-crest-derived pigment cell fate. Development 126, 3757–3767.
[14] Yang, X.J. et al. (2013) A novel zebrafish xenotransplantation model for study of glioma stem cell invasion. PLoS One 8, e61801.
[15] Nasevicius, A. and Ekker, S.C. (2000) Effective targeted gene 'knockdown' in zebrafish. Nat. Genet. 26, 216–220.
[16] Altschul, S.F., Gish, W., Miller, W., Myers, E.W. and Lipman, D.J. (1990) Basic local alignment search tool. J. Mol. Biol. 215, 403–410.
[17] Beissbarth, T. and Speed, T.P. (2004) GOstat: find statistically overrepresented gene ontologies within a group of genes. Bioinformatics 20, 1464–1465.
[18] Varambally, S. et al. (2005) Integrative genomic and proteomic analysis of prostate cancer reveals signatures of metastatic progression. Cancer Cell 8, 393–406.
[19] Yu, Y.P. et al. (2004) Gene expression alterations in prostate cancer predicting tumor aggression and preceding development of malignancy. J. Clin. Oncol. 22, 2790–2799.
[20] Chandran, U.R. et al. (2007) Gene expression profiles of prostate cancer reveal involvement of multiple molecular pathways in the metastatic process. BMC Cancer 7, 64.

[21] Kim, J.H. et al. (2011) Deep sequencing reveals distinct patterns of DNA methylation in prostate cancer. Genome Res. 21, 1028–1041.

[22] Altschul, S.F., Madden, T.L., Schaffer, A.A., Zhang, J., Zhang, Z., Miller, W. and Lipman, D.J. (1997) Gapped BLAST and PSI-BLAST: a new generation of protein database search programs. Nucleic Acids Res. 25, 3389–3402.

[23] Fossey, S.C., Kuroda, S., Price, J.A., Pendleton, J.K., Freedman, B.I. and Bowden, D.W. (2000) Identification and characterization of PRKCBP1, a candidate RACK-like protein. Mamm. Genome 11, 919–925.

[24] Eichmuller, S., Usener, D., Dummer, R., Stein, A., Thiel, D. and Schadendorf, D. (2001) Serological detection of cutaneous T-cell lymphoma-associated antigens. Proc. Natl. Acad. Sci. USA 98, 629–634.

[25] Panagopoulos, I. et al. (2013) Fusion of ZMYND8 and RELA genes in acute erythroid leukemia. PLoS One 8, e63663.

[26] Park, J., Betel, D., Gryfe, R., Michalickova, K., Di Nicola, N., Gallinger, S., Hogue, C.W. and Redston, M. (2002) Mutation profiling of mismatch repair-deficient colorectal cncers using an in silico genome scan to identify coding microsatellites. Cancer Res. 62, 1284–1288.

[27] Wang, F., Yamauchi, M., Muramatsu, M., Osawa, T., Tsuchida, R. and Shibuya, M. (2011) RACK1 regulates VEGF/Flt1-mediated cell migration via activation of a PI3K/Akt pathway. J. Biol. Chem. 286, 9097–9106.

[28] Du, J., Xu, R., Hu, Z., Tian, Y., Zhu, Y., Gu, L. and Zhou, L. (2011) PI3K and ERK-induced Rac1 activation mediates hypoxia-induced HIF-1alpha expression in MCF-7 breast cancer cells. PLoS One 6, e25213.

[29] Yoshiji, H. et al. (1999) Protein kinase C lies on the signaling pathway for vascular endothelial growth factor-mediated tumor development and angiogenesis. Cancer Res. 59, 4413–4418.

[30] Xia, P. et al. (1996) Characterization of vascular endothelial growth factor's effect on the activation of protein kinase C, its isoforms, and endothelial cell growth. J. Clin. Investig. 98, 2018–2026.

[31] Clément-Duchêne, C. et al. (2012) A phase II study of enzastaurin in combination with erlotinib in patients with previously treated advanced non-small cell lung cancer. Lung Cancer 78, 57–62.

[32] Gray, J.E., Altiok, S., Alexandrow, M.G., Walsh, F.W., Chen, J., Schell, M.J., Tai, D.F. and Bepler, G. (2013) Phase 2 randomized study of enzastaurin (LY317615) for lung cancer prevention in former smokers. Cancer 119, 1023–1032.

[33] Grønberg, B.H. et al. (2012) A placebo-controlled, randomized phase II study of maintenance enzastaurin following whole brain radiation therapy in the treatment of brain metastases from lung cancer. Lung Cancer 78, 63–69.

[34] Wei, X.W., Zhang, Z.R. and Wei, Y.Q. (2013) Anti-angiogenic drugs currently in Phase II clinical trials for gynecological cancer treatment. Expert Opin. Investig. Drugs 22, 1181–1192.

[35] Karaman, M.W. et al. (2008) A quantitative analysis of kinase inhibitor selectivity. Nat. Biotechnol. 26, 127–132.

[36] Mochly-Rosen, D., Das, K. and Grimes, K.V. (2012) Protein kinase C, an elusive therapeutic target? Nat. Rev. Drug Discov. 11, 937–957.

[37] Stebbins, E.G. and Mochly-Rosen, D. (2001) Binding specificity for RACK1 resides in the V5 region of beta II protein kinase C. J. Biol. Chem. 276, 29644–29650.

[38] Kim, J., Choi, Y.L., Vallentin, A., Hunrichs, B.S., Hellerstein, M.K., Peehl, D.M. and Mochly-Rosen, D. (2008) Centrosomal PKCbetaII and pericentrin are critical for human prostate cancer growth and angiogenesis. Cancer Res. 68, 6831–6839.

[39] Westendorf, J.J. and Koka, S. (2004) Identification of FHOD1-binding proteins and mechanisms of FHOD1-regulated actin dynamics. J. Cell. Biochem. 92, 29–41.

[40] Westendorf, J.J., Mernaugh, R. and Hiebert, S.W. (1999) Identification and characterization of a protein containing formin homology (FH1/FH2) domains. Gene 232, 173–182.

[41] Chabannes, E., Fauconnet, S., Bernardini, S., Wallerand, H., Adessi, G. and Bittard, H. (2001) Protein kinase C signalling pathway is involved in the regulation of vascular endothelial growth factor expression in human bladder transitional carcinoma cells. Cell. Signal. 13, 585–591.

[42] Amadio, M., Bucolo, C., Leggio, G.M., Drago, F., Govoni, S. and Pascale, A. (2010) The PKCbeta/HuR/VEGF pathway in diabetic retinopathy. Biochem. Pharmacol. 80, 1230–1237.

[43] Drabsch, Y., He, S., Zhang, L., Snaar-Jagalska, B.E. and Ten Dijke, P. (2013) Transforming growth factor-beta signalling controls human breast cancer metastasis in a zebrafish xenograft model. Breast Cancer Res. 15, R106.

[44] Folkman, J. (1976) The vascularization of tumors. Sci. Am. 234 (58–64), 70–73.